LHCb-CONF-2011-055
September 27, 2011

Measurement of the ratio of branching fractions $\mathcal{B}(B^0 \to K^{*0}\gamma)/\mathcal{B}(B_s^0 \to \phi\gamma)$ with the LHCb experiment at $\sqrt{s} = 7$ TeV

The LHCb Collaboration [1]

Abstract

The ratio of branching ratios of the radiative B decays $B^0 \to K^{*0}\gamma$ and $B_s^0 \to \phi\gamma$ has been measured using 340.1 pb^{-1} of pp collisions at a centre of mass energy of $\sqrt{s} = 7$ TeV taken with the LHCb detector. The obtained value for the ratio is $1.52 \pm 0.14(\text{stat}) \pm 0.10(\text{syst}) \pm 0.12(f_s/f_d)$. Using the HFAG value for $\mathcal{B}(B^0 \to K^{*0}\gamma)$, $\mathcal{B}(B_s^0 \to \phi\gamma)$ has been found to be $(2.8 \pm 0.5) \times 10^{-5}$.

[1] Conference report prepared for Lepton-Photon 2011, Mumbai. Contact authors: Olivier Deschamps, Albert Puig

1 Introduction

Radiative decays of the B_d meson were first observed by the CLEO collaboration in 1993 [1], through the $B^0 \to K^{*0}\gamma$ decay mode. In 2007, the Belle collaboration reported the first observation of the equivalent decay mode in the B_s sector, $B_s \to \phi\gamma$. In the Standard Model (SM), the amplitude of these $b \to s\gamma$ penguin transitions is dominated by a virtual intermediate top quark coupling to a W boson. Extensions of the SM predict new heavy particles that may propagate virtually within the loop and modify the dynamics of the transition. Therefore, these radiative modes are promising laboratories that could reveal the presence of new phenomena beyond the SM with the precise measurement of the branching ratios, asymmetries or angular distributions.

The current world average of the branching fractions (denoted as $\mathcal{B}$) are a combination [2] of measurements made by BABAR [3], Belle [4, 5] and CLEO [6]:

$$\begin{aligned} \mathcal{B}(B^0 \to K^{*0}\gamma)\ (\text{HFAG}) &= (4.33 \pm 0.15)\ \times 10^{-5} \\ \mathcal{B}(B_s^0 \to \phi\gamma)\ (\text{HFAG}) &= (5.7^{+2.1}_{-1.8})\ \times 10^{-5} \end{aligned} \tag{1}$$

providing the current best value for the ratio between branching fractions as

$$\frac{\mathcal{B}(B^0 \to K^{*0}\gamma)}{\mathcal{B}(B_s^0 \to \phi\gamma)} = 0.7 \pm 0.3 \tag{2}$$

The most recent theoretical predictions regarding $B \to V\gamma$ decays come from NNLO calculations using SCET [7],

$$\begin{aligned} \mathcal{B}(B^0 \to K^{*0}\gamma)\ (\text{NNLO}) &= (4.3 \pm 1.4)\ \times 10^{-5} \\ \mathcal{B}(B_s^0 \to \phi\gamma)\ (\text{NNLO}) &= (4.3 \pm 1.4)\ \times 10^{-5} \end{aligned} \tag{3}$$

and therefore, taking into account uncertainty correlations, a value compatible with Eq. 2 is found:

$$\frac{\mathcal{B}(B^0 \to K^{*0}\gamma)}{\mathcal{B}(B_s^0 \to \phi\gamma)} = 1.0 \pm 0.2, \tag{4}$$

The experimental results are both in agreement with and more precise (in the case of $B \to K^{*0}\gamma$) than SM predictions, which suffer from large uncertainties from hadronic factors. The experimental value of $\mathcal{B}(B_s^0 \to \phi\gamma)$ is affected by very large uncertainty due to limited statistics.

This note presents a preliminary measurement of the ratio of branching fractions of the $B^0 \to K^{*0}\gamma$ and $B_s^0 \to \phi\gamma$ decays using ~ 340 pb^{-1} of data from the 2011 run of the LHCb detector [8].

2 Data sample

The analysis is performed using an integrated luminosity of 340.1 ± 11.9 pb^{-1} of $\sqrt{s} = 7$ TeV pp-collision data taken with the LHCb detector in the March-June 2011 run, in

which all detector components and relevant trigger lines were fully operational and stable. Events corresponding to each of the channels are collected using the following trigger selection:

- at the hardware level (L0 trigger): an E_T cut of 2.5 GeV is applied to the photon candidate;
- in the High Level Trigger (HLT): as a first step, an inclusive selection is applied by requiring one of the daughter tracks of the vector meson (K^{*0}/ϕ) to have a p_T larger than 1.7 GeV/c. This transverse momentum threshold is reduced to 1.2 GeV/c when the photon candidate is found to have a very large p_T in excess of 4.2 GeV/c.
  As a second step a loose *exclusive* selection is performed, based on :
  - the Impact Parameter (IP) —the minimum distance between the track and its associated primary vertex— and χ^2 of the track associated to the K and π
  - the vertex quality and mass window of the intermediate vector meson
  - the IP, mass window and direction between the flight direction and momentum of the reconstructed B candidate.

3 Selection

The offline selection of both the $B^0 \to K^{*0}\gamma$ and $B_s^0 \to \phi\gamma$ decays is performed with the strategy of maximizing the cancellation of systematic uncertainties when performing the ratio. Therefore, the selection criteria and cut values are very similar, as can be seen in Tab. 1, and have been optimized to maximize the signal significance.

The first step in the selection consists of forming $K^{*0} \to K^+\pi^-$ ($\phi \to K^+K^-$) candidates from pairs of opposite-charged tracks identified as K and π which come from a good common vertex ($\chi^2 < 9$) and with an IP χ^2 higher than 25. Both tracks are required to have p_T higher than 500 MeV/c and a good track quality (track χ^2/dof).

The photons are reconstructed from the energy clusters in the Electromagnetic Calorimeter (ECAL) that cannot be associated with any charged trajectory [8]. The additional information provided by the Scintillator-Pad and Preshower calorimetric detectors, located upstream of the ECAL, are combined with the track-cluster matching estimator to provide a photon identification variable, γ-ID [9]. Photon candidates are selected with an $E_T > 2600$ GeV/c requirement. At such high transverse energy, the photon pairs from the neutral π decays are likely to be reconstructed as a single electromagnetic cluster within the ECAL granularity. In order to reduce the background contamination from high energy π^0 decays a π^0/γ separation tool has been designed, by combining several variables based on the shower shape of the ECAL cluster.

The selected vector mesons and photons are combined to build B candidates. The helicity structure imposed by the signal decays is exploited to remove π^0-related back-

		$B^0 \to K^{*0}\gamma$	$B_s^0 \to \phi\gamma$
track IP χ^2		> 25	> 25
track p_T	(MeV)	> 500	> 500
K PID_K		> 5	> 5
K $\mathrm{PID}_K - \mathrm{PID}_p$		> 2	> 2
π PID_K		< 0	-
meson ΔM_{PDG}	(MeV)	< 50	< 9
meson vertex χ^2		< 9	< 9
γ E_T	(MeV)	> 2600	> 2600
γ-ID		> 0.25	> 0.25
π^0/γ separation		> 0.5	> 0.5
$p_{T,B}$	(MeV)	> 3000	> 3000
B IP χ^2		< 9	< 9
B helicity		< 0.8	< 0.8
B isolation $\Delta\chi^2$		> 0.5	> 0.5

Table 1: *Summary of the selection cuts performed in the selection of both decay channels. The cuts are divided in sections, which in order are: track cuts, particle identification cuts (PID), vector meson cuts, photon cuts and B candidate cuts.*

ground, since one expects the helicity angle[2] θ_H to follow a $\sin^2\theta_H$ distribution for signal and a $\cos^2\theta_H$ for the $B_{d(s)} \to K^{*0}(\phi)\pi^0$ background, while the combinatorial background is flat [10].

In addition, in order to further reduce the specific background contamination coming from partially reconstructed multibody B decays, a vertex isolation criteria is applied by rejecting the $B_{d(s)} \to K^*(\phi)\gamma$ candidates when any additional track from the event can be added to the decay vertex with an increase of the vertex χ^2 smaller than 0.5 units.

4 Background studies

A detailed study of the background contamination has been done, and the systematics and corrections for each contribution have been calculated. Four background categories have been considered, and their contributions are summarized in Tab. 2:

- *Combinatorial background.* The mass shape of the combinatorial background has been extracted from the sidebands of the K^{*0} ($|\Delta M(K^{*0})| > 100$ MeV/c^2) using a dedicated monitoring selection with an enlarged mass window. Its B candidate mass distribution has been found to be consistent with an exponential shape. Further-

[2]The helicity angle θ_H is defined as the angle between one daughter of the vector meson and the reconstructed B meson, both evaluated in the rest frame of the vector meson.

more, there is a good matching between the decay constant found in the sideband fit and that found when performing the full fit in the signal area.

- *Contamination from high energy* π^0. Charmless $B \to hh\pi^0$ meson decays with branching fractions of $\infty\prime^{-\triangledown}$ can produce a dangerous contamination to both the $B_d \to K^{*0}(K^+\pi^-)\gamma$ and $B_s \to \phi(K^+K^-)\gamma$ signals in the case of misidentification of π^0 as γ. Their contribution has been modelled using Monte Carlo simulation and is found to not exceed the $\sim 1\%$ level. Therefore, the signal yields of the fit have been corrected by the amounts shown in Tab. 2.

- *Contamination from partially reconstructed B decays.* Partial reconstruction of B decays can provide a possible source of dangerous background contaminating the signal on the low mass side. The multi-hadrons radiative decays from both the charged modes, like $B^+ \to K^{*0}\pi^+\gamma$, $B^+ \to \phi K^+\gamma$, and the neutral modes, like $B^0 \to K^{*0}\gamma\pi^0$, $B_s \to \phi\gamma K^0$, with a total Branching Ratio of few 10^{-5}, partially exhibit the signal topology in their final state. Morever, the partial reconstruction of a decay fragment from the (possibly charmed) $B \to (K^{*0}\pi^0)X$ decays may also contribute with a significantly larger branching ratio. The partially reconstructed B decays have been studied at the simulation level for several modes. It produces a peaking shape around 4.6 GeV/c^2 with a large tail in the signal region. Such background is strongly reduced thanks to several selection criteria such that the K^{*0}/ϕ-vertex isolation or the $B_{d(s)}$ direction angle. The total branching ratio contributing to this background is however potentially large and the amplitude of the contamination is therefore essentially unknown. The impact of the background model on the signal yield extraction has been studied by adding such a contribution in the fit, with a shape fixed from the Monte Carlo studies while the amplitude is allowed to vary freely. Related systematic uncertainty has been extracted.

- *Signal crossfeeds.* The so-called *signal cross-feed* category actually consists of three contributions, which have been detailed in the last section of Tab. 2. Firstly, a correction due to the irreductible contamination from $B_s \to K^{*0}\gamma$ to $B^0 \to K^{*0}\gamma$ has been added. Crossfeed due to the kaon-pion misidentifcation between $B^0 \to K^{*0}\gamma$ and $B_s^0 \to \phi\gamma$ has been also studied using Monte Carlo, and only the $B_s^0 \to \phi\gamma$ contamination into $B^0 \to K^{*0}\gamma$ is found to be relevant. Finally, multiple candidates in signal events have been studied, and no suitable way to reduce their contribution has been found, so a correction to the yields is also added.

5 Fit procedure

The fit procedure is designed to extract simultaneously the yields for $B^0 \to K^{*0}\gamma$ and $B_s^0 \to \phi\gamma$ using an extended unbinned maximum likelihood method. The fit contains an ad-hoc exponential parametrization for the non-peaking background, while the peaking

	$B^0 \to K^{*0}\gamma$		$B_s^0 \to \phi\gamma$	
contribution	correction	systematics	correction	systematics
$B_d \to K^+\pi^-\pi^0$	-1.3%	$\pm 0.4\%$	—	$\mathcal{O}(10^{-4})$
$B_s \to K^+\pi^-\pi^0$	-0.5%	$\pm 0.5\%$	—	$\mathcal{O}(10^{-4})$
$B_s \to K^+K^-\pi^0$	—	$\mathcal{O}(10^{-4})$	-1.3%	$\pm 1.3\%$
background model	—	$\pm 3.8\%$	—	$\pm 3.8\%$
$B_s \to K^+\pi^-\gamma$	-0.8%	$\pm 0.4\%$	—	—
$\phi\gamma \iff K^{*0}\gamma$ cross-feed	-0.4%	$\pm 0.2\%$	—	$\mathcal{O}(10^{-4})$
multiple candidates	-0.45%	$\pm 0.2\%$	-0.3%	$\pm 0.2\%$
Total	-3.5%	$\pm 3.9\%$	-1.6%	$\pm 4.0\%$

Table 2: *Correction factor and corresponding systematic uncertainty affecting the signal yields induced by the specific background contaminations, the combinatorial background shape modelling and the signal cross-feed. The total systematic uncertainty is obtained by summing quadratically the individual contributions.*

background and the cross-feed contributions are taken into account in the signal extraction and the systematics as discussed in the previous section.

Following Monte Carlo studies, the signal for both B mesons is parametrized with a Crystal-Ball (CB) distribution in order to account for possible losses in the photon energy due to the fiducial volume of the calorimeter. While mean position and width of the gaussian component of the CB are expected to be different between data and MC, and thus are left free, the values of the n and α parameters are extracted from Monte Carlo. In the simultaneous fit, the difference between the positions of the B and B_s peaks (μ_B and μ_{B_s}) is kept fixed at the PDG value, 86.8 MeV/c^2, in order to reduce the number of free parameters and help with the low-statistics $B_s^0 \to \phi\gamma$ fit.

The results of the fits on 340.1 pb^{-1} of data are shown in Fig. 1 and enumerated in Tab. 3.

6 Extraction of the ratio of branching fractions

The ratio of branching ratios is calculated from the number of fitted events as shown in Eq. 5, where the ϵ parameters represent the total efficiencies, including acceptance, trigger, reconstruction and selection.

$$\frac{\mathcal{B}(B^0 \to K^{*0}\gamma)}{\mathcal{B}(B_s^0 \to \phi\gamma)} = \frac{\mathcal{Y}_{B^0 \to K^{*0}\gamma}}{\mathcal{Y}_{B_s^0 \to \phi\gamma}} \frac{\mathcal{B}(\phi \to K^+K^-)}{\mathcal{B}(K^* \to K^+\pi^-)} \frac{f_s}{f_d} \frac{\epsilon_{B_s^0 \to \phi\gamma}}{\epsilon_{B^0 \to K^{*0}\gamma}} \tag{5}$$

The extraction of the different ratios is as follows:

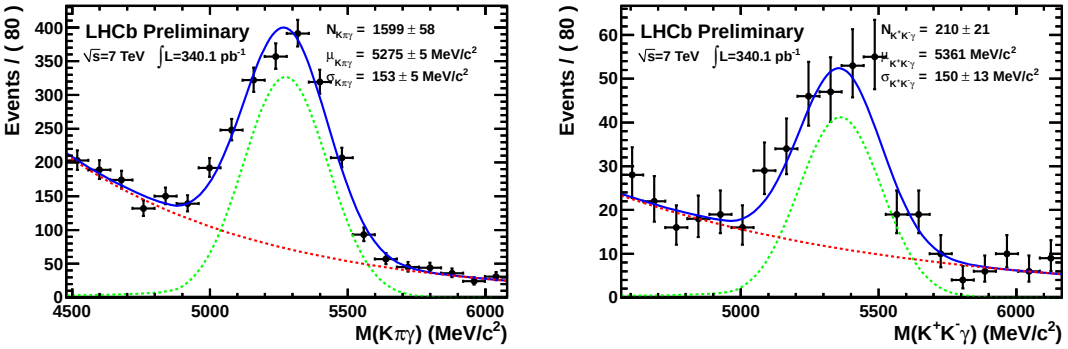

Figure 1: *Results of the fits for the $B^0 \to K^{*0}\gamma$ (left) and $B_s^0 \to \phi\gamma$ (right). The black points represent the data and the fit result is represented as a solid blue line. The signal is fitted with a Crystal-Ball function (dashed green line) and the background is described as an exponential (dashed red line).*

parameter	value	units	fit status
μ_{B^0}	5275 ± 5	MeV/c^2	free
δ_m	86.6	MeV/c^2	fixed from PDG
σ_{B^0}	153 ± 5	MeV/c^2	free
$\sigma_{B_s^0}$	150 ± 13	MeV/c^2	free
n	0.7	—	fixed from MC
α	2.461	—	fixed from MC
$\tau_{B^0}^{\text{bkg}}$	-1.03 ± 0.05	GeV/c^2	free
$\tau_{B_s^0}^{\text{bkg}}$	-0.92 ± 0.14	GeV/c^2	free
N_{B^0}	1599 ± 58	—	free
$N_{B_s^0}$	210 ± 21	—	free
N_{bkg,B^0}	1777 ± 60	—	free
N_{bkg,B_s^0}	288 ± 23	—	free

Table 3: *Summary of fixed and fitted parameters for signal shape (first section), background shape (second section) and yields (third section) with their values after the fit on real data. The B meson mass difference, $\delta_m = M(B_s) - M(B_d^0)$, is fixed from the PDG value, while the Crystal-Ball tail parameters for the signal model,(α, n) are fixed from Monte-Carlo simulation.*

- The yield ratio is extracted from the fits in Tab. 3 after applying the background corrections from Tab. 2 to the $B^0 \to K^{*0}\gamma$ and $B_s^0 \to \phi\gamma$ yields.
- The vector mesons decay rate into the visible modes is extracted from the Particle Data Book [11].
- The ratio f_s/f_d is taken from the combined LHCb measurement, which has a 7.5%

uncertainty [12].

- The efficiencies are split into trigger, acceptance and reconstruction, and selection. The ratio of efficiencies between the two channel can be written as in Eq. 6

$$\frac{\epsilon^{B_s^0\to\phi\gamma}}{\epsilon^{B^0\to K^{*0}\gamma}} = \frac{\epsilon^{B_s^0\to\phi\gamma}_{\text{Trigger}}}{\epsilon^{B^0\to K^{*0}\gamma}_{\text{Trigger}}} \frac{\epsilon^{B_s^0\to\phi\gamma}_{\text{Acceptance\&Reco}}}{\epsilon^{B^0\to K^{*0}\gamma}_{\text{Acceptance\&Reco}}} \frac{\epsilon^{B_s^0\to\phi\gamma}_{\text{SelNoPID}}}{\epsilon^{B^0\to K^{*0}\gamma}_{\text{SelNoPID}}} \frac{\epsilon^{B_s^0\to\phi\gamma}_{\text{SelPID}}}{\epsilon^{B^0\to K^{*0}\gamma}_{\text{SelPID}}} \tag{6}$$

  The ratio of trigger, acceptance and reconstruction, and selection (without PID) efficiencies are extracted from Monte Carlo signal samples, while the PID efficiencies are extracted directly from data using PID tables[3]. The results for the ratios of efficiencies are shown in Tab. 4.

	ratio
trigger	1.057 ± 0.008
acceptance and reconstruction	1.303 ± 0.006
selection (no PID)	0.814 ± 0.004
PID	0.931 ± 0.005
Global	1.044 ± 0.012

Table 4: *Summary of intermediate efficiency ratios needed to compute the global efficiency ratio defined in Eq. 6.*

Intermediate results for the ratios in Eq. 5 are detailed in Tab. 5. Combining this information we obtain:

$$\frac{\mathcal{B}(B^0\to K^{*0}\gamma)}{\mathcal{B}(B_s^0\to\phi\gamma)} = 1.52 \pm 0.14(\text{stat}) \tag{7}$$

where the quoted statistical error comes only from the ratio of yields obtained in the fit.

	contribution
r_ϵ	1.044 ± 0.012
$r_{\text{vector meson }\mathcal{B}}$	0.735 ± 0.008
f_s/f_d	0.267 ± 0.020
$r_\mathcal{Y}$	7.4 ± 0.7

Table 5: *Summary of contributions to the ratio of branching ratios as defined in Eq. 5.*

[3]The PID tables, provided by the PID group, provide efficiencies for given PID cuts for kaons and pions in bins of p, p_T and η. These tables are determined using $D\to K\pi$ control samples.

7 Systematic uncertainties

The main sources for systematic uncertainties are

- *Monte Carlo statistics.* Source of uncertainty in the trigger, acceptance and reconstruction, and selection (no PID) efficiencies.

- *Reconstruction efficiency for hadrons.* The systematics error due to the uncertainty in the hadron reconstruction efficiency is evaluated assuming that the material budget is known within 20%. Studies have shown [13] that there is an average difference of 20% interaction lengths between pions and kaons. Assuming this difference, and adding the fact that the material budget in LHCb is 0.2 hadronic interaction lengths, the uncertainty in the material budget gives a systematic uncertainty of 0.4% on the measured ratio.

- *Center of the vector meson mass window.* In the selection, the center for the mass window is taken to be the PDG value of the mass for the vector mesons. Due to small misalignments, the mass peak position differs between data and Monte Carlo, and neither corresponds exactly to the expected PDG value. Therefore, we estimate the related systematic uncertainty by varying the central value of the cut on the mass window from the PDG value to the position found in data.

- *Reliability of the Monte Carlo distributions.* Variables that differ between data and Monte Carlo are mainly the IP χ^2 and the vertex isolation $\Delta\chi^2$. To deal with the systematics associated with these two variables, we have reweighted the data with the MC distribution and recalculated the ratio.

- *PID.* The systematics associated with the PID tables is evaluated comparing the results obtained using the Monte Carlo PID tables —obtained in the same way as the data ones— and the results obtained by directly applying the cuts on the signal sample. In addition, statistical error of the PID tables is considered.

- *Fit.* The for the $B^0 \to K^{*0}\gamma$ and $B_s^0 \to \phi\gamma$ decays from Tab. 2 are added in quadrature.

Their values are summarized in Tab. 6. Note that no systematics are associated to the photon reconstruction due to the fact that the reconstruction in both decays is identical.

8 Results and conclusions

In 340 pb^{-1} of pp collisions at a centre of mass energy of $\sqrt{s} = 7$ TeV the ratio of branching fractions between $B^0 \to K^{*0}\gamma$ and $B_s^0 \to \phi\gamma$ has been measured to be

$$\frac{\mathcal{B}(B^0 \to K^{*0}\gamma)}{\mathcal{B}(B_s^0 \to \phi\gamma)} = 1.52 \pm 0.14(\text{stat}) \pm 0.10(\text{syst}) \pm 0.12(f_s/f_d) \tag{8}$$

source	σ/ratio
MC statistics of trigger ratio	0.8 %
Acceptance and reconstruction	0.7 %
Selection (no PID)	1.2 %
PID efficiencies	2.7 %
background	5.6 %
hadronization fractions	1.0 %
overall uncertainty	6.5 %
f_s/f_d	7.9 %
Total	10.2 %

Table 6: *Summary of contributions to the systematic uncertainty, where σ/ratio stands for the relative uncertainty on the ratio from each of the sources. Note that f_s/f_d is not included in the overall uncertainty as it will be given separately in the final result. The total is calculated as a quadratic sum of the overall uncertainty and the f_s/f_d systematic.*

This results is compatible within 1.6 standard deviations with the theory prediction.

Combining the ratio of branching fractions in Eq. 8 with the World Average measurement for the $\mathcal{B}(B^0 \to K^{*0}\gamma\ )$ from Eq. 1, we obtain the most precise value for the $\mathcal{B}(B_s^0 \to \phi\gamma\ )$,

$$\mathcal{B}(B_s^0 \to \phi\gamma) = (2.8 \pm 0.5) \times 10^{-5} \tag{9}$$

which agrees within 1.6 standard deviations with the previous experimental measurement.

Acknowledgments

We express our gratitude to our colleagues in the CERN accelerator departments for the excellent performance of the LHC. We thank the technical and administrative staff at CERN and at the LHCb institutes, and acknowledge support from the National Agencies: CAPES, CNPq, FAPERJ and FINEP (Brazil); CERN; NSFC (China); CNRS/IN2P3 (France); BMBF, DFG, HGF and MPG (Germany); SFI (Ireland); INFN (Italy); FOM and NWO (Netherlands); SCSR (Poland); ANCS (Romania); MinES of Russia and Rosatom (Russia); MICINN, XUNGAL and GENCAT (Spain); SNSF and SER (Switzerland); NAS Ukraine (Ukraine); STFC (United Kingdom); NSF (USA). We also acknowledge the support received from the ERC under FP7 and the Region Auvergne.

References

[1] CLEO, R. Ammar et al., *Evidence for penguin-diagram decays: First observation of* $B \to K^*(892)\gamma$, *Phys. Rev. Lett.* **71** (Aug, 1993) 674–678.

[2] Heavy Flavor Averaging Group, D. Asner et al., *Averages of b-hadron, c-hadron, and* τ*-lepton Properties*, TT arXiv:hep-ex/1010.1589.

[3] BaBar, B. Aubert et al., *Measurement of Branching Fractions and CP and Isospin Asymmetries in* $B \to K^*(892)\gamma$ *Decays*, *Phys. Rev. Lett.* **103** (2009) 211802, [TT arXiv:hep-ex/0906.2177].

[4] Belle, J. Wicht et al., *Observation of* $B_s^0 \to \phi\gamma$ *and Search for* $B_s^0 \to \gamma\gamma$ *Decays at Belle*, *Phys. Rev. Lett.* **100** (2008) 121801, [TT arXiv:hep-ex/0712.2659].

[5] Belle, M. Nakao et al., *Measurement of the* $B \to K^*\gamma$ *branching fractions and asymmetries*, *Phys. Rev. D* **69** (Jun, 2004) 112001.

[6] CLEO, T. E. Coan et al., *Study of Exclusive Radiative B Meson Decays*, *Phys. Rev. Lett.* **84** (Jun, 2000) 5283–5287.

[7] A. Ali, B. D. Pecjak, and C. Greub, $B \to V\gamma$ *Decays at NNLO in SCET*, *Eur. Phys. J.* **C55** (2008) 577–595, [TT arXiv:hep-ph/0709.4422].

[8] LHCb Collaboration, A. Augusto Alves Jr et al., *The LHCb Detector at the LHC*, *JINST* **3** (2008), no. S08005.

[9] O. Deschamps, F. Machefert, M.-H. Schune, G. Pakhlova, and I. Belyaev, *Photon and Neutral Pion reconstruction*, LHCb Public Note LHCb-2003-091, CERN, Sep, 2003.

[10] L. Shchutska, A. Golutvin, and I. Belyaev, *Study of radiative penguin decays* $B \to K^{*0}\gamma$ *and* $B_s \to \phi\gamma$ *at LHCb*, LHCb Public Note LHCb-2007-030. CERN-LHCb-2007-030, CERN, Geneva, May, 2007.

[11] Particle Data Group, K. Nakamura et al., *Review of particle physics*, *J.Phys.G* **G37** (2010) 075021.

[12] LHCb Collaboration, *Average* f_s/f_d *b-hadron production fraction for 7 TeV pp collisions*, LHCb Analysis Note LHCb-ANA-2011-065, CERN, Jul, 2011.

[13] S. Miglioranzi and G. Corti, *Material interaction cross section studies*, LHCb Internal Note LHCb-INT-2011-002, CERN-LHCb-INT-2011-002, CERN, Geneva, Jan, 2011.